Simulation of hydraulic fracturing process by using peridynamics

†Shuhui Li*, Fan Wu, Shasha Qiu, Zeyang Feng

Department of Engineering Mechanics, The State key Laboratory of Structural Analysis for Industrial Equipment, Dalian University of Technology, Dalian, Liaoning 116024, P.R.China.

*Presenting author: shuhuili@dlut.edu.cn
†Corresponding author: shuhuili@dlut.edu.cn

Abstract

A non-local bond-based peridynamic method is employed to simulate the hydraulic fracture process since it involves propagation of massive cracks in a brittle solid where crack branching and interaction present. Traditional numerical methods (e.g. XFEM) developed specially for cracks are awkward to simulate hydraulic fracture process because of its huge amount of cracks. Instead, peridynamic as a recently developed theory of solid mechanics replaces the partial differential equations of the classical continuum theory with integral equations. Hence, its basic equations are valid everywhere, regardless of continuities. This prominent advantage enables peridynamic to simulate hydraulic fracture process. This paper applies the peridynamic method to simulate the hydraulic fracturing of shale, containing horizontal well fracking with multiple perforations and initial natural cracks. A new scheme of tracing crack path and applying hydraulic fracture pressure is proposed. And some preliminary 2D results are presented to illustrate the validity of the proposed method. The numerical results show that hydraulic fracture cracks can restrain each other when they get close. With different angles of initial natural cracks, the crack pattern presents big difference.

Keywords: Peridynamic, Hydraulic fracture, Massive cracks, Fragmentation, Crack propagation

Introduction

Shale gas as a new energy source receives increasingly attentions these years. British Petroleum expects the shale gas revolution that has already transformed the U.S. natural gas market to continue apace. However, shale gas exploration faces many severe problems because of the depth of shale format, lean ore, environment pollution, etc [1]. To increase output, a mainstream technique called hydraulic fracture was developed. Hydraulic fracture, also known as fracking, injects high-pressure fluid into rocks deep underground, inducing the release of fossil fuels. Hence, using modern computer to simulate hydraulic fracture and consequently giving guidance on practical engineering is especially important.

Computational simulation is developed rapidly on account of its economic advantage. It's rather challenge to simulate problems involving massive cracks propagation, branching and interaction, such as hydraulic fracture process. Traditional numerical method such as finite element method, based on classical continuum mechanics which is the most popular adopted in commercial software, for example, has the assumption of continuity. This assumption, which contradicts the fact of physics, leads to the invalidation when it comes to discontinuity. Other numerical method such as extend finite element method specially developed for cracks also suffers severe problem dealing with massive cracks problem as fracking.

In light of the inadequacies of local classical continuum mechanics theories, the peridynamic theory, which is nonlocal, was introduced by Silling [2] in an attempt to deal with the

discontinuities. Basically, the peridynamics theory is a reformulation of the equation of motion in solid mechanics that is better suited for modeling bodies with discontinuities, such as cracks [3]. Consequently, peridynamic model is adopted in this paper to simulate hydraulic fracture, which many researchers have proved reliable [4]-[7].

This paper is organized as follows: section 2 introduces the basic theory of peridynamic model. Hydraulic fracture process is briefly introduced as well. The numerical implement of hydraulic fracture is discussed in section 3, containing the hydraulic fracture pressure applied by crack path tracing scheme developed in this paper. In section 4, several numerical results are presented. And conclusion is given in section 5.

Peridynamic model of hydraulic fracturing

Peridynamic basic theory

Peridynamic theory is a non-local theory which assumes that an arbitrary material point in a body interacts with other material points within its range, called horizon, as shown in Fig 1. It can be regarded as a continuum version of molecular dynamics. Each material point follows Newton's Second Law in the form of

$$\rho(\boldsymbol{x})\ddot{\boldsymbol{u}}(\boldsymbol{x},t)=\int_H \boldsymbol{f}\left(\boldsymbol{u}(\boldsymbol{x},t)-\boldsymbol{u}(\boldsymbol{x}',t),\boldsymbol{x}-\boldsymbol{x}'\right)dH+\boldsymbol{b}(\boldsymbol{x},t) \qquad (1)$$

in which $\boldsymbol{\rho}$ is the material density. $\boldsymbol{u}(\boldsymbol{x},t)$ is the displacement of point $\boldsymbol{x}$. $\boldsymbol{b}$ is the applied force in the form of body force. H denotes the range of point $\boldsymbol{x}$ can act on, named horizon. All others points in a certain material point's horizon together is called this material point's family. The interaction between two family points is defined as a bond. $\boldsymbol{f}$ describes the internal force between each couple of material points, called pairwise force function. It has the dimension of force per volume squared.

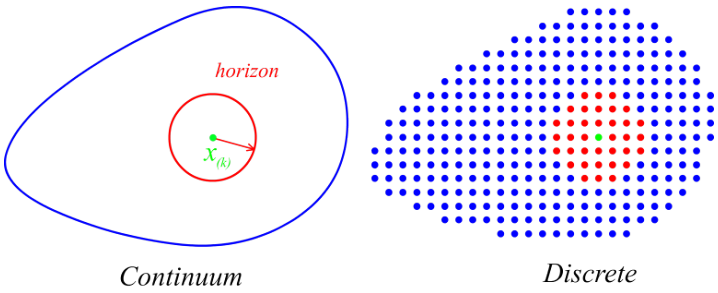

Figure 1. Peridynamic theory

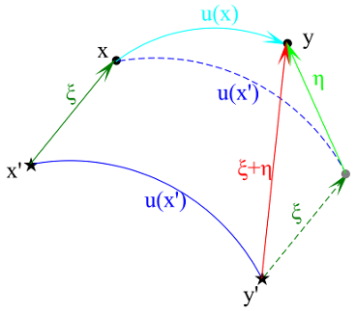

Figure 2. Relationship between relative position vector and relative displacement vector

Pairwise force function can be derived from bond's micro-potential ω. In micro-elastic material, for example:

$$\boldsymbol{f} = (\boldsymbol{\eta}, \boldsymbol{\xi}) = \frac{\partial \omega(\boldsymbol{\eta}, \boldsymbol{\xi})}{\partial \boldsymbol{\eta}} \tag{2}$$

$\boldsymbol{\xi} = \boldsymbol{x} - \boldsymbol{x}'$ is the initial bond vector called relative position vector. $\boldsymbol{\eta} = \boldsymbol{u} - \boldsymbol{u}'$ is the deformed bond vector called relative displacement vector as shown in Figure 2. In this paper, a PMB (prototype micro-elastic brittle) material [8] is considered, defined by

$$\omega(\eta, \xi) = \frac{c(\xi) s^2(\xi)}{2} \tag{3}$$

where $\xi = |\boldsymbol{\xi}|, \eta = |\boldsymbol{\eta}|$ are the magnitudes of the corresponding vectors. s is the bond stretch which represents the elongation of bond defined as

$$s = \frac{\zeta - \xi}{\xi} \tag{4}$$

$\zeta = |\boldsymbol{\zeta}| = |\boldsymbol{\xi} + \boldsymbol{\eta}|$ is the bond vector in the current reference configuration. $c(\xi)$ is a material parameter describes the stiffness of a single bond, called micro-modulus.

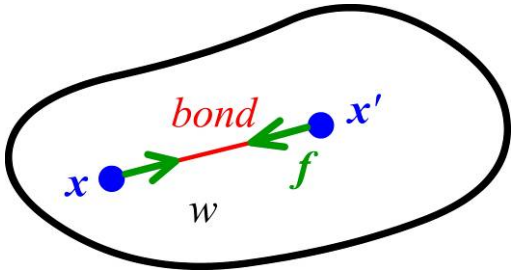

Figure 3. Peridynamic bond and micro-potential

Additionally, the pairwise force function for PMB material is obtained by differentiating the micro-potential

$$f = |\boldsymbol{f}| = cs \tag{5}$$

By Equaling strain energy density in the classical theory and peridynamic theory this peridynamic material parameter can be associated with bulk modulus k in classical theory. For linear elastic material, consider a large homogeneous body under isotropic extension

$$\eta = s\xi \qquad \forall \xi \tag{6}$$

Thus

$$f = cs = c\eta / \xi \tag{7}$$

It follows that

$$\omega = \frac{c\eta^2}{2\xi} = \frac{cs^2\xi}{2} \tag{8}$$

The strain energy density for peridynamic theory can be obtained by integrating the micro-potential associated within a certain point's horizon

$$W = \frac{1}{2}\int_{H_x} \omega(\boldsymbol{\eta}, \boldsymbol{\xi}) dV_\xi \tag{9}$$

1/2 means that each bond's strain energy density is shared by two connected points. Therefore, strain energy density for peridynamic theory can be obtained. For example in 3D

$$W_{PD} = \frac{1}{2}\int_{H_x} \omega(\boldsymbol{\eta}, \boldsymbol{\xi}) dV_\xi = \frac{1}{2}\int_0^\delta \left(\frac{cs^2\xi}{2} \right) dV_\xi \tag{10}$$

where δ is the radius of horizon. $W_{PD} = W_{CM}$ leads to

$$\begin{cases} c = \dfrac{6E}{\pi\delta^3(1-\nu)} & p-\sigma \\ c = \dfrac{6E}{\pi\delta^3(1-2\nu)(1+\nu)} & p-\varepsilon \\ c = \dfrac{12E}{\pi\delta^4} & 3D \end{cases} \tag{11}$$

where E is the elastic modulus, ν is the possion ratio [9]. In the bond-based peridynamic theory

$$\nu = \begin{cases} \dfrac{1}{3} & 2D \\ \dfrac{1}{4} & 3D \end{cases} \tag{12}$$

Failure is introduced at bond level. A bond breaks when its elongation s exceeds the critical relative elongation s_0

$$\begin{cases} \boldsymbol{f} = cs\dfrac{\boldsymbol{\xi}+\boldsymbol{\eta}}{|\boldsymbol{\xi}+\boldsymbol{\eta}|} & s \le s_0 \\ \boldsymbol{f} = \boldsymbol{0} & s > s_0 \end{cases} \tag{13}$$

Once a bond is broken, it stays broken. That means bonds can't heal. And it makes the model historical dependent.

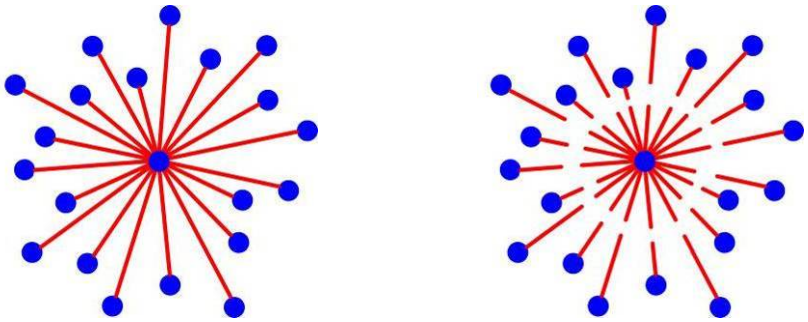

Figure 4. Damage status

Additionally, a quantity describing the damage status of a certain point is defined by

$$\varphi(x,t) = 1 - \frac{\int_H \mu(\mathbf{x},t,\xi)dV_h}{\int_H dV_h} \tag{14}$$

Simulation of hydraulic fracture via peridynamic

The hydraulic fracture process is shown in Figure 5. Fracking fluid is injected after perforating on the wall of horizontal well. Horizontal well is the one of the most widely used technique in shale gas production process because of its long length in horizontal direction. The difficulty in simulating horizontal well fracking is obvious: it involves massive cracks. Thus peridynamic theory mentioned above is applied for simulation in this paper.

Material parameters used are adopted from Nongan oil shale field in Jilin Province of China as listed in Table 1 below. Perforations are applied as initial cracks by cutting off all the bonds crossing the initial crack paths.

Table 1. Shale parameter

E(Gpa)	Density(kg/m^3)	Possion ratio	s_0
19.03	2400	1/3	0.00003

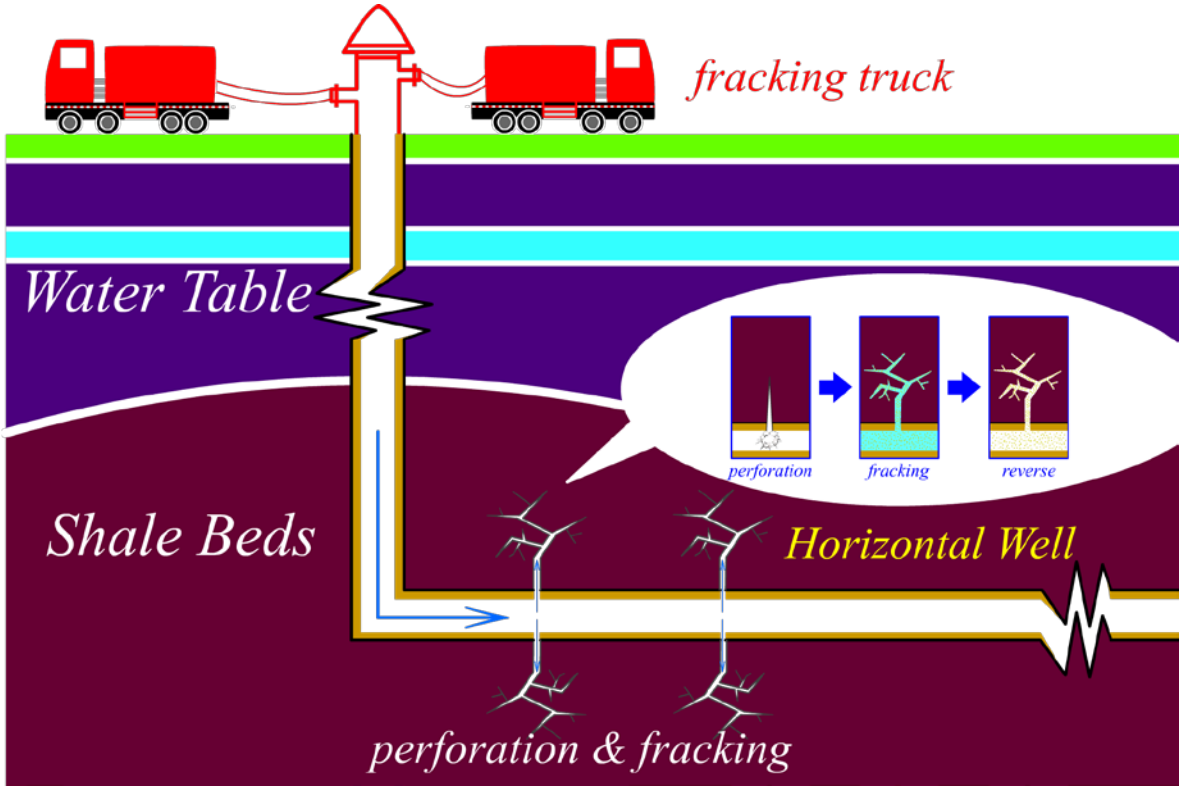

Figure 5. Schematic of hydraulic fracture process

Numerical implementation

Time integration

Velocity-Verlet algorithm [10] is adopted here as time integration, which is an explicit method. The Velocity-Verlet algorithm is

$$\begin{aligned} \dot{\boldsymbol{u}}_{n+\frac{1}{2}} &= \dot{\boldsymbol{u}}_n + \frac{\Delta t}{2}\ddot{\boldsymbol{u}}_n \\ \boldsymbol{u}_{n+1} &= \boldsymbol{u}_n + \Delta t\dot{\boldsymbol{u}}_{n+\frac{1}{2}} \\ \dot{\boldsymbol{u}}_{n+1} &= \dot{\boldsymbol{u}}_{n+\frac{1}{2}} + \frac{\Delta t}{2}\ddot{\boldsymbol{u}}_{n+1} \end{aligned} \tag{15}$$

where $\ddot{\boldsymbol{u}}$, $\dot{\boldsymbol{u}}$ and $\boldsymbol{u}$ are acceleration, velocity and displacement respectively.

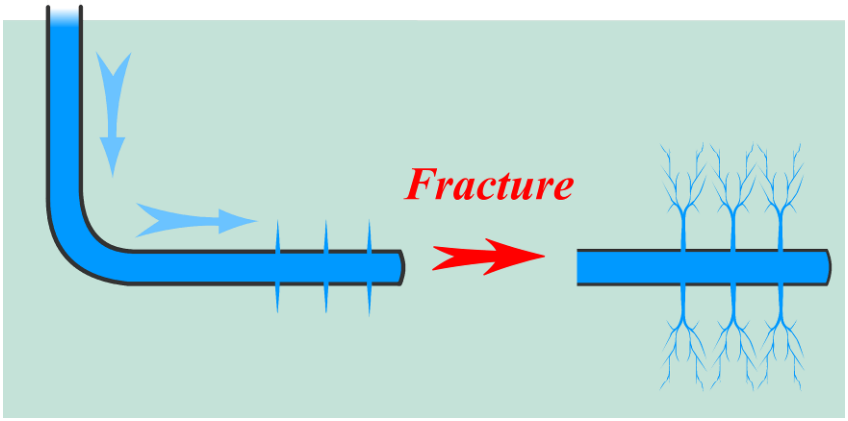

Figure 6. Schematic of crack network caused by hydraulic fracture

Hydraulic fracture pressure applied by crack path tracing scheme

One of the most important features of hydraulic fracture is that hydraulic fracture pressure needs to be applied on both initial cracks and new born cracks, as shown as in Fig 6. Thus a new scheme is proposed in this paper to trace the hydraulic fracture crack paths in peridynamic model, and the corresponding normal directions can also be obtained. Cracks might be very chaotic when cracks branching, especially fragmentation occurred, as Fig 7. To find the effective material points on crack paths, points with damage at certain level are adopted in this paper:

$$0.35 < \varphi < 0.50 \tag{16}$$

And the normal direction of a certain point on the crack path illustrated in Fig 8 is calculated by weighted average of its associated bonds' lengths

$$\alpha_b(\xi) = \sum_{i=1}^{\infty} p_i \left(\frac{\xi}{\Delta x} \right)^{i-1} \tag{17}$$

in which p_i is the coefficient of fitting polynomial. Consequently the corresponding direction of a certain point i can be obtained by

$$\begin{aligned} \cos\theta_i &= \sum_{b}^{\infty} \alpha_b \cdot \cos\theta_b \\ \sin\theta_i &= \sum_{b}^{\infty} \alpha_b \cdot \sin\theta_b \end{aligned} \tag{18}$$

where the subscript b donate the bond's number associated with point i.

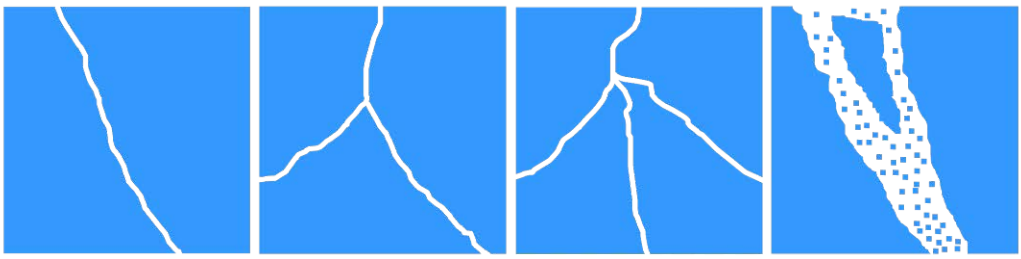

Figure 7. Schematic of several kinds of crack path

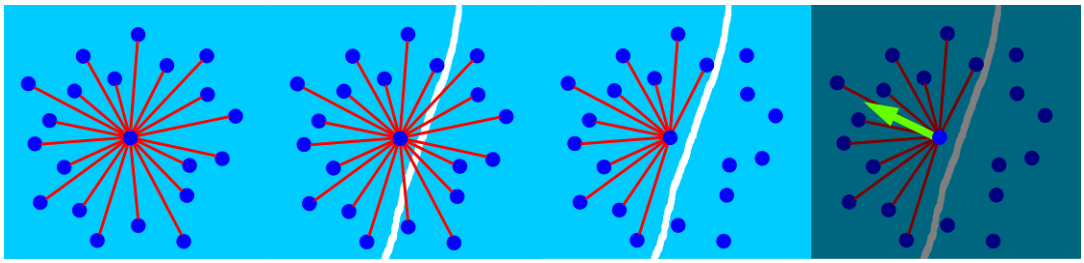

Figure 8. Determination of hydraulic fracture pressure direction

Results

In this section, longitudinal section of horizontal well is studied as shown in Figure 9. Half of the longitudinal section is omitted because of its symmetry. The domain is $40m \times 20m$, with perforations on the bottom wall of horizontal well. The hydraulic fracture pressure applied is shown in Figure 10 which is increasing over time. Time step is $\Delta t = 10^{-5} s$, perforation depth is $a = 1.0m$, and the mesh size is $\Delta x = 0.1m$.

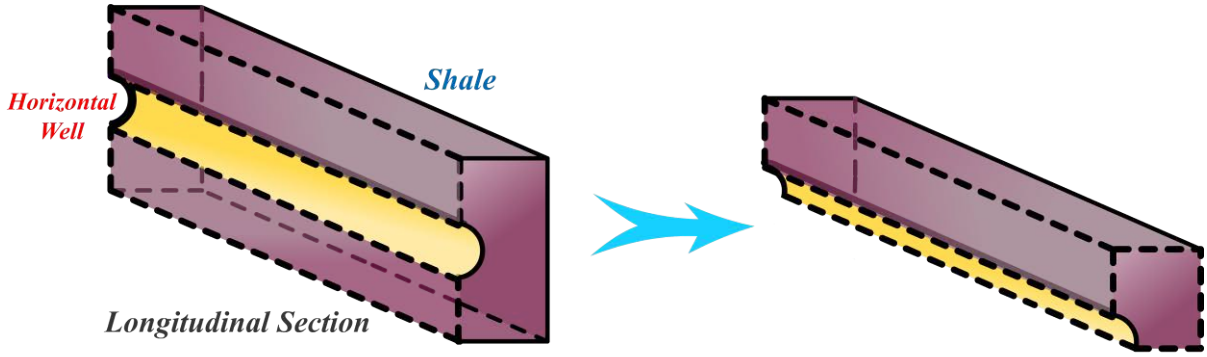

Figure 9. Schematic of longitudinal section of horizontal well

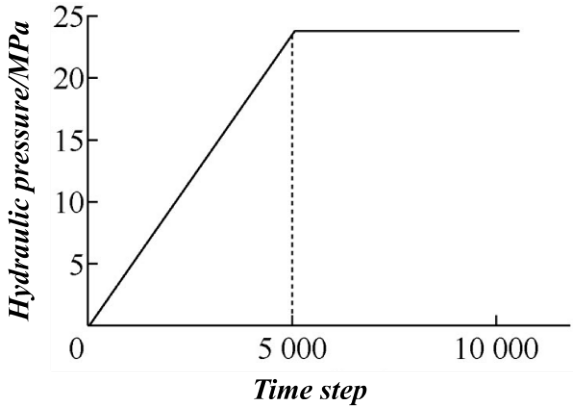

Figure 10. Fracking load

Numerical results of different numbers of perforations

The influence of perforations is studied here. One, two and three perforations on the wall of horizontal wells are set, as in Figure 11. The simulation results are shown in Figure 12. Cracks branching and secondary branching path occur. It proves that peridynamic model is convenient to deal with hydraulic fracture problem.

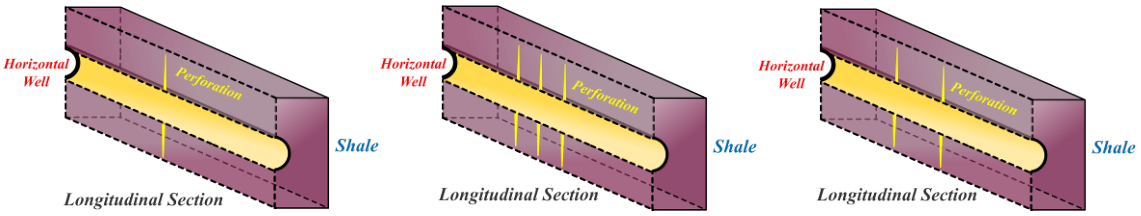

Figure 11. Schematic of horizontal well with different numbers of perforations

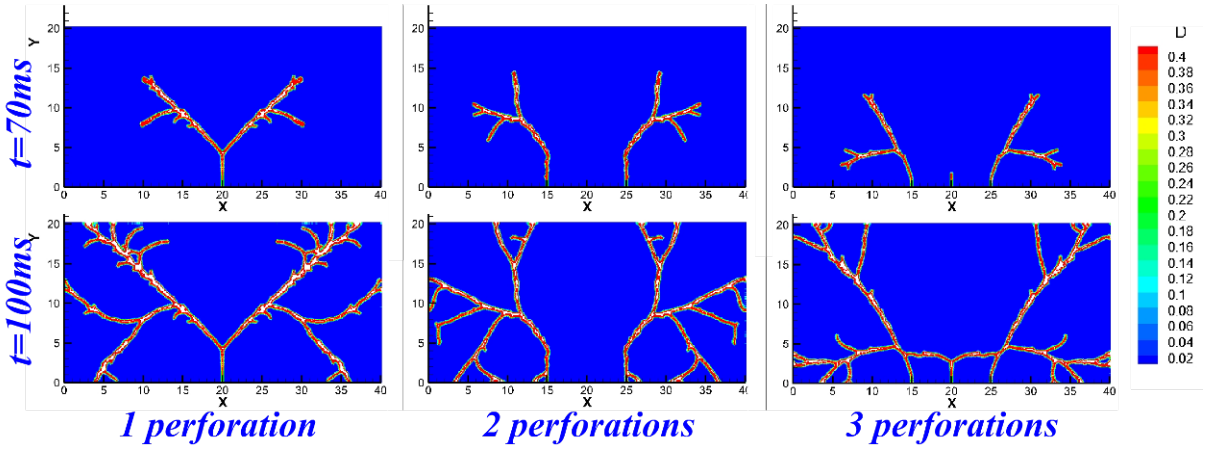

Figure 12. Different numbers of perforations fracking result

Additionally, it illustrates that in the hydraulic fracture process cracks can be restrained by each other when distance between cracks reduces during propagation. Figure 13 shows the relationship between time step and crack paths length which is most concerned. The crack paths lengths are represented by the numbers of material points applied in hydraulic fracture pressure. An interesting phenomenon is that the single perforation crack paths length reaches the maximum at last and nearly the same order of magnitude as the others all the time. Thus it proves that simply addition of perforation number in a certain area can't increase the crack path length proportionally. It's not wise to set perforations too dense to get better fracking results.

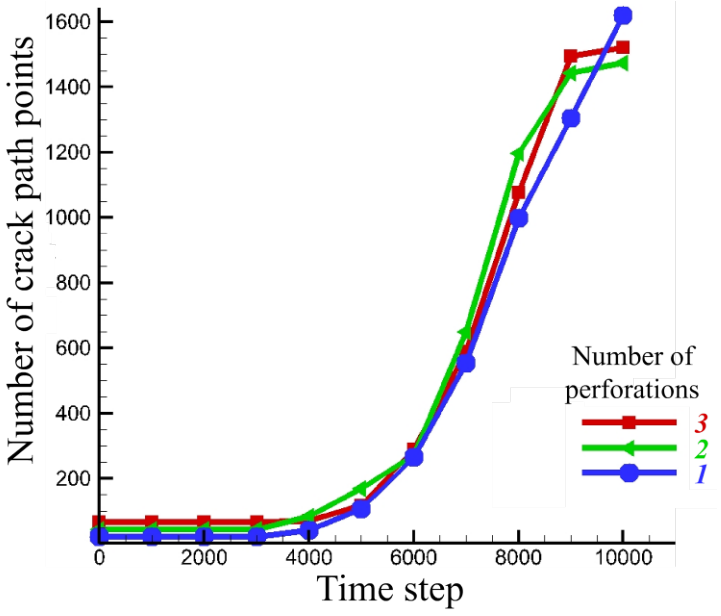

Figure 13. Relationship between time and crack path length

Numerical results of various angles of initial natural cracks

Furthermore, cases of two perforations with different angle of initial natural cracks fracking are investigated to discuss the influence of initial natural cracks. The computational domain is same as above. Fracking pressure applied, mesh size, perforation depth, time step are same as the previous case, too.

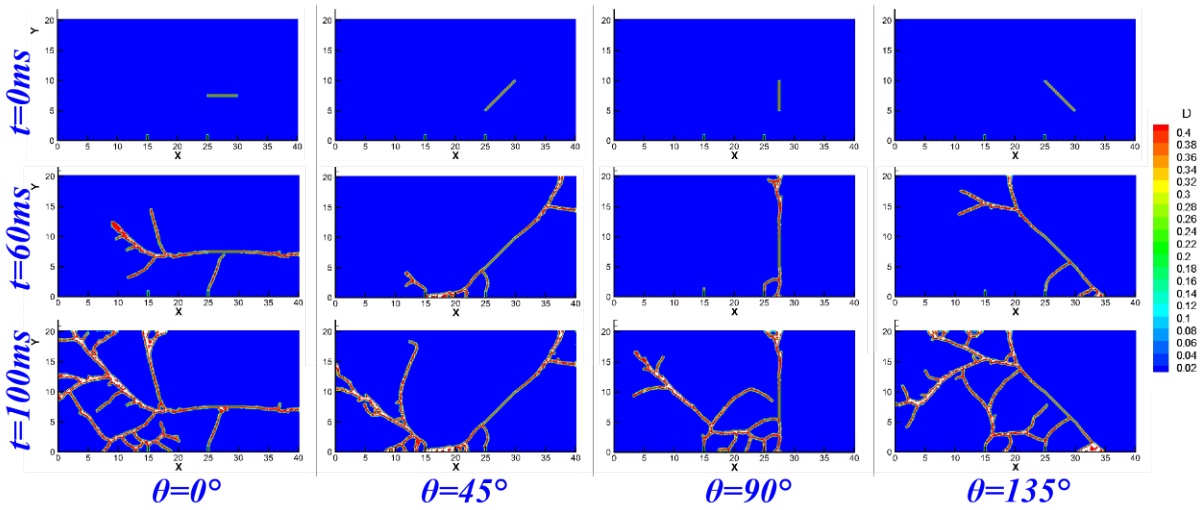

Figure 14. Various angles of initial natural cracks fracking result

The results are shown above in Figure 14. It reveals different angles of initial natural cracks influence the crack results remarkably. As shown in Figure 15 at $t = 100ms$ 0° natural crack case reaches the maximum by 1496 crack path points, while case with 45° natural crack gets the minimum crack path points by 1000. Since the shale is lamellar structure full of natural cracks with certain angles, investigation of the geological structure would be particularly important.

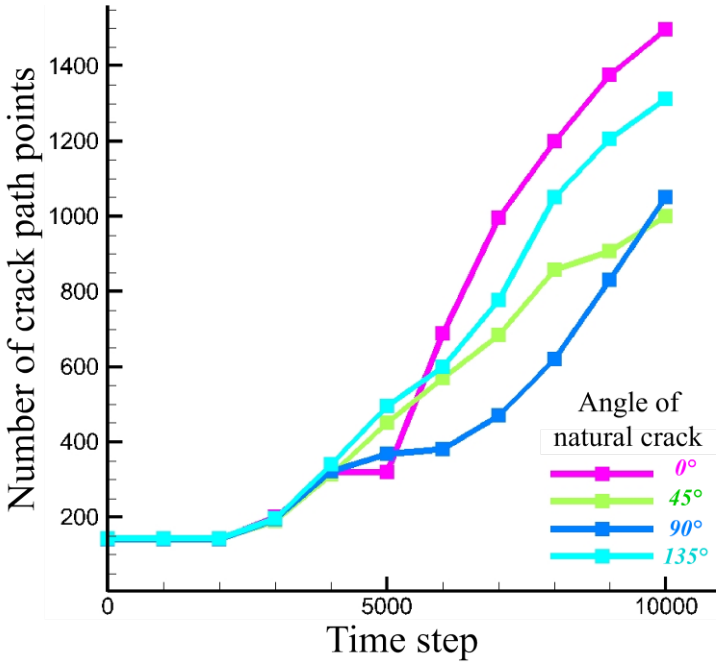

Figure 15. Relationship between time and crack path length

Conclusions

Peridynamic is a powerful method to deal with the problem involving massive cracks. In this paper, hydraulic fracture process is simulated by peridynamic model we developed. With the crack path tracing scheme we developed, crack branching and coalescence are observed in the numerical results which prove it is convenient and suitable for hydraulic fracture problems. The results also revealed that hydraulic fracture perforation numbers at a certain area are closely associated with crack patterns. And perforations restrain the cracks propagation when they set close enough. That means increasing the number of perforation simply in a certain area can't guarantees the increasing of crack proportionally. Besides, initial natural cracks distances remarkably influence the fracking results. Therefore, investigation of geologic structure is significant meaningful for hydraulic process before engineering construction.

Acknowledgement

The authors are pleased to acknowledge the support of this work by Science Challenge Project (No. JCKY2016212A502), the National Key Research and Development Program of China (2016YFC1402705, 2016YFC1402706), the National Natural Science Foundation of China (11372066, 11232003), the Fundamental Research Funds for the Central Universities (DUT15LK07), the open funds of the state key laboratory of water resources and hydropower engineering science (2015SGG03), the open funds of the state key laboratory of Geohazard Prevention and Geoenvironment Protection (SKLGP2016K007).

References

[1] Bowker, K. A. (2007) Barnett Shale gas production, Fort Worth Basin: Issues and discussion, Aapg Bulletin, **91**,523-533.

[2] Silling, S. A.. (2000) *Reformulation of elasticity theory for discontinuities and long-range forces*, Journal of the Mechanics & Physics of Solids **48,**175-209.

[3] Lee, J., Liu, W., and Hong, J. W. (2005) *Impact fracture analysis enhanced by contact of peridynamic and finite element formulations*, International Journal of Impact Engineering, **87**,108-119.

[4] Wu, F., Li, S. H., Duan, Q. L. and Li, X. K. (2017) *Application of the Method of Peridynamics to the Simulation of Hydraulic Fracturing Process*, Proceedings of the 7th International Conference on Discrete Element Methods. Springer Singapore.

[5] Wu F, Li S, Duan Q, Li X, and Zhang H. W. (2017) Numerical simulation of hydraulic fracturing process based on the method of peridynamics , Computer Aided Engineering, **26**(1),1-6

[6] Nadimi, S., Miscovic, I. and Mclennan, J. (2016) *A 3D peridynamic simulation of hydraulic fracture process in a heterogeneous medium*, Journal of Petroleum Science & Engineering, **145**,444-452.

[7] Ouchi, H., Katiyar, A., Foster, J. T. and Sharma, M. M. (2015) *A Peridynamics Model for the Propagation of Hydraulic Fractures in Heterogeneous, Naturally Fractured Reservoirs*, SPE Hydraulic Fracturing Technology Conference, Texas.

[8] Silling, S. A. and Askari, E. (2005) *A meshfree method based on the peridynamic model of solid mechanics*. Computers & Structures, **83**(17–18),1526-1535.

[9] Shojaei, A., Mudric, T., Zaccariotto, M. and Galvanetto, U. (2016) *A coupled meshless finite point/Peridynamic method for 2D dynamic fracture analysis*. International Journal of Mechanical Sciences, **119**,419-431.

[10] Hairer E, Lubich C and Wanner G. (2003) *Geometric numerical integration illustrated by the Störmer-Verlet method*. Acta Numerica, **12**(12), 399--450.